THE JOURNAL OF BIOLOGICAL CHEMISTRY VOL. 286, NO. 8, pp. 6080–6084, February 25, 2011

A Na^+-translocating Pyrophosphatase in the Acetogenic Bacterium *Acetobacterium woodii*[*]

Received for publication, October 8, 2010, and in revised form, November 25, 2010 Published, JBC Papers in Press, December 20, 2010, DOI 10.1074/jbc.M110.192823

Eva Biegel and Volker Müller[1]

From the Department of Molecular Microbiology and Bioenergetics, Institute of Molecular Biosciences, Johann Wolfgang Goethe University Frankfurt/Main, Max-von-Laue-Strasse 9, 60438 Frankfurt, Germany

The anaerobic acetogenic bacterium *Acetobacterium woodii* employs a novel type of Na^+-motive anaerobic respiration, caffeate respiration. However, this respiration is at the thermodynamic limit of energy conservation, and even worse, in the first step, caffeate is activated by caffeyl-CoA synthetase, which hydrolyzes ATP to AMP and pyrophosphate. Here, we have addressed whether or not the energy stored in the anhydride bond of pyrophosphate is conserved by *A. woodii.* Inverted membrane vesicles of *A. woodii* have a membrane-bound pyrophosphatase that catalyzes pyrophosphate hydrolysis at a rate of 70–120 milliunits/mg of protein. Pyrophosphatase activity was dependent on the divalent cation Mg^{2+}. In addition, activity was strictly dependent on Na^+ with a K_m of 1.1 mM. Hydrolysis of pyrophosphate was accompanied by $^{22}Na^+$ transport into the lumen of the inverted membrane vesicles. Inhibitor studies revealed that $^{22}Na^+$ transport was primary and electrogenic. Next to the Na^+-motive ferredoxin:NAD^+ oxidoreductase (Fno or Rnf), the Na^+-pyrophosphatase is the second primary Na^+-translocating enzyme in *A. woodii.*

The anaerobic acetogenic bacterium *Acetobacterium woodii* is the prime example for an organism that has based its bioenergetics on Na^+ instead of H^+ (1–4). The energy-conserving pathways such as carbonate respiration (Wood-Ljungdahl pathway) (5, 6) are Na^+-motive; the F_1F_0-ATP synthase uses Na^+ as coupling ion (7, 8); and the flagellar motor is powered by an electrochemical sodium ion gradient (9). In addition, *A. woodii* is able to grow in the apparent absence of an electrochemical proton gradient, indicating that the growth-essential secondary transport systems are also driven by $\Delta\mu_{Na^+}$.[2]

A. woodii not only grows by CO_2 reduction, but it can also reduce the double bond of certain phenylacrylates, such as caffeate, in a process called caffeate respiration (3, 10–13), in which caffeate is reduced to hydrocaffeate, and a Na^+ gradient is established across the cytoplasmic membrane that drives ATP synthesis (11). In this anaerobic respiration, oxidation of sugars or hydrogen yields reduced ferredoxin that is reoxidized by a membrane-bound Na^+-translocating ferredoxin:NAD^+ oxidoreductase (Fno/Rnf) (14, 15). This is the only coupling site known in caffeate respiration, and thermodynamic calculations show that this reaction allows for the transport of 1–2 mol of Na^+. Assuming that 3–4 mol of Na^+/mol of ATP are translocated, 3–4 mol of caffeate have to be reduced to synthesize 1 mol of ATP. Given this unfavorable energy balance, it was surprising to see that the electron acceptor caffeate is activated to caffeyl-CoA prior to its reduction by NADH via a hypothetical caffeyl-CoA reductase-Etf complex. Caffeate activation is catalyzed by an AMP-dependent caffeyl-CoA synthetase that hydrolyzes ATP to AMP and PP_i (35). Thus, two energy-rich phosphate bonds have to be invested. Here, we have addressed whether or not some energy may be saved by conserving the energy of the PP_i bond in the form of an electrochemical ion (Na^+) gradient across the membrane. To search for such an activity, we have used an inverted membrane vesicle system of *A. woodii*, $^{22}Na^+$, as a tracer and pyrophosphate as an energy source.

EXPERIMENTAL PROCEDURES

Growth of Cells and Preparation of Vesicles—A. woodii (DSM 1030) was grown under anaerobic conditions using 20 mM fructose as substrate as described (5, 7). The preparation of vesicles was done as described but slightly modified. For preparation of vesicles, the growth medium was supplemented with 420 mM sucrose and 8.1 mM $MgSO_4$. 5 liters of medium were inoculated (4%), and the absorbance was followed at 600 nm. At A_{600} = 0.7–0.9, 70 μg of penicillin G/ml were added to the medium to induce protoplast formation. During further incubation, *A. woodii* formed protoplasts as monitored by microscopic observations. After 20 h, the culture consisted almost entirely of spherical forms that were highly sensitive to low osmolarity. These protoplasts were harvested aerobically by centrifugation (6250 × *g*, 20 min, 4 °C) and washed in 25 mM Pipes (sodium-free)/KOH buffer (pH 6.8) containing 25 mM $MgSO_4$ and 420 mM sucrose. After washing the protoplasts, they were resuspended in a total volume of 300 ml and incubated with lysozyme (1 mg/ml) for 30 min at room temperature. The protoplasts were centrifuged (6250 × *g*, 20 min, 4 °C) and resuspended in 10–20 ml of Pipes/KOH buffer (pH 6.8) containing 25 mM $MgSO_4$ and 420 mM sucrose. These protoplasts were passed through a French pressure cell at 41 megapascals and centrifuged three times (4500 × *g*, 35 min, 4 °C). The resulting supernatant (*i.e.* crude vesicles) was centrifuged further by ultracentrifugation (120,000 × *g*, 40 min, 4 °C). The pellet was washed in Pipes/KOH buffer (pH 6.8) containing 25 mM $MgSO_4$ and 420 mM sucrose and centrifuged again. The resulting pellet was resus-

* This work was supported by a grant from the Deutsche Forschungsgemeinschaft (SFB 807).
[1] To whom correspondence should be addressed. Tel.: 49-69-7982-9507; Fax: 49-69-7982-9306; E-mail: vmueller@bio.uni-frankfurt.de.
[2] V. Müller, unpublished data.

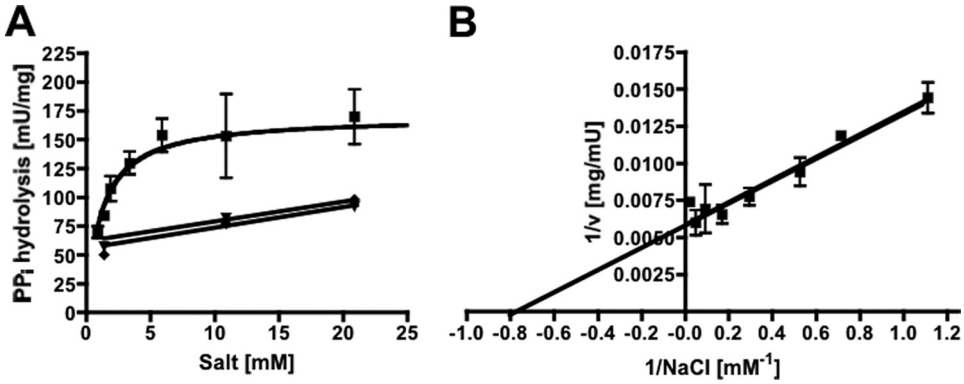

FIGURE 1. **Na^+ dependence of PP_i hydrolysis.** *A*, PP_i hydrolysis was determined in membrane vesicles in 25 mM Pipes/KOH buffer (pH 6.8) containing 25 mM $MgSO_4$, 420 mM sucrose, and varying NaCl concentrations. The effect of NaCl (*squares*), KCl (*diamonds*), or LiCl (*inverted triangles*) on PP_i hydrolysis. *B*, the corresponding Lineweaver-Burk plot for NaCl is shown. Data from two independent experiments are shown.

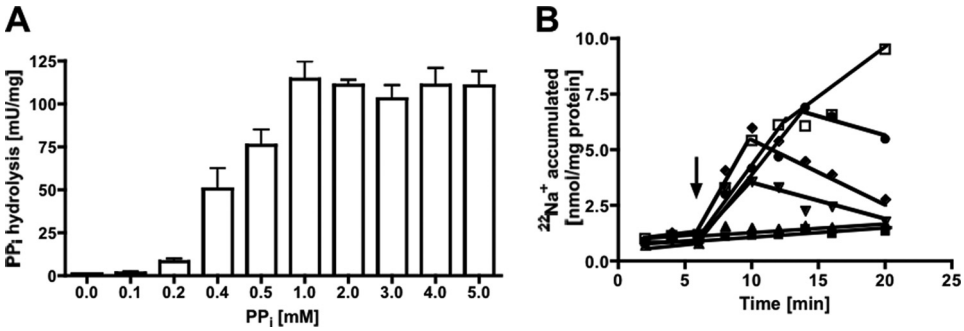

FIGURE 2. **Dependence of PP_i hydrolysis and $^{22}Na^+$ transport on the PP_i concentration.** Membrane vesicles (protein concentrations of 1.1 mg/ml in hydrolysis assay and 3.3 mg/ml in transport) in 25 mM Pipes/KOH buffer (pH 6.8) containing 25 mM $MgSO_4$, 420 mM sucrose, and 1.9 mM NaCl showed PP_i hydrolysis activity (*A*) and $^{22}Na^+$ transport depending on the PP_i concentration (*B*): 0 mM (*closed squares*), 0.1 mM (*triangles*), 0.5 mM (*inverted triangles*), 1 mM (*diamonds*), 2.5 mM (*circles*), 5 mM PP_i (*open squares*). The *arrow* indicates the addition of PP_i.

pended in the same buffer in a volume of 3 ml. Protein concentrations were determined by the method of Bradford (16).

PP_i Hydrolysis—Pyrophosphatase (PPase)[3] activity was determined by measuring the released phosphate using a method described by Heinonen and Lathi (17).

Measurement of Na^+ Translocation—The experiments were performed under aerobic conditions in Pipes/KOH buffer (pH 6.8) containing 25 mM $MgSO_4$ and 420 mM sucrose as described (7). The sodium and protein concentrations used are indicated. In a 1.5-ml Eppendorf cup, the vesicles, buffer, supplements (17 μM valinomycin, 1 mM *N*,*N*′-dicyclohexylcarbodiimide, NaCl, and 150 mM KCl), and ^{22}NaCl (final activity of 0.5 μCi/ml) were combined and incubated at 30 °C for 120 min to assure equilibration of $^{22}Na^+$ before the reaction was started with potassium pyrophosphate (final concentration of 1 mM or as indicated). 100 μM *N*,*N*,*N*,*N*′-tetracyclohexyl-1,2-phenylenedioxydiacetamide (ETH 2120) and 3,5-di-*tert*-butylhydroxybenzylidenemalonitrile (SF 6847) were added 6 min before the addition of PP_i. 100-μl samples were withdrawn from the cup and passed over a column (0.5 × 3.2 cm) of Dowex 50-WX8 (100–200-mesh) (7). The vesicles were collected by washing the column with 1 ml of 420 mM sucrose. The radioactivity in the eluate was determined by liquid scintillation counting. For elucidating the effect of Mg^{2+} on the transport activity, the vesicles were prepared in the same buffer except that $MgSO_4$ was omitted. $MgSO_4$ and EDTA were added from stock solutions before the addition of ^{22}NaCl.

Determination of Na^+ Concentration—The Na^+ concentration in the buffer was determined with an Orion 84-11 ROSS sodium electrode (Thermo Electron Corp., Witchford, UK) as described (18).

RESULTS

Inverted membrane vesicles (IMVs) of *A. woodii* prepared in Pipes/KOH buffer (pH 6.8) that also contained 25 mM $MgSO_4$, 420 mM sucrose, and 1.9 mM NaCl were incubated at 30 °C. Upon the addition of PP_i, it was hydrolyzed with a rate of 70–120 milliunits/mg (1 unit corresponding to 1 μmol of PP_i/min at 1.9 mM NaCl). PP_i hydrolysis was dependent on the external Na^+ concentration. When no sodium was added to the assay, an activity of 68–74 milliunits/mg was measured (resulting from residual Na^+ in the buffer and vesicles), but increasing Na^+ concentrations led to increasing activities in a Michaelis-Menten-type fashion (Fig. 1*A*). The double-reciprocal plot is shown in Fig. 1*B*, and a K_m of 1.1 ± 0.4 mM and a V_{max} of 170 ± 12 milliunits/mg of protein were obtained. KCl and LiCl had only a marginal stimulatory effect. Pyrophosphate hydrolysis was dependent on the pyrophosphate concentration. Highest activities were obtained at 1 mM PP_i (Fig. 2*A*). Pyrophosphate hydrolysis was accompanied by $^{22}Na^+$ transport into the vesicles (Fig. 2*B*). As expected, $^{22}Na^+$ transport increased with the pyrophosphate concentration. Also, at

[3] The abbreviations used are: PPase, pyrophosphatase; IMV, inverted membrane vesicle.

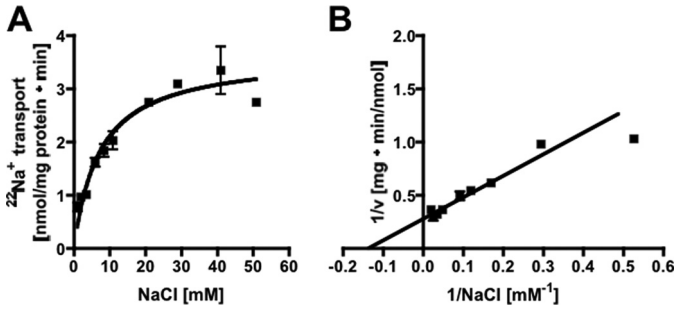

FIGURE 3. **Na^+ dependence of PP_i-dependent transport activity.** Membrane vesicles (protein concentration of 3.6 mg/ml) were incubated in 25 mM Pipes/KOH buffer (pH 6.8) containing 25 mM $MgSO_4$, 420 mM sucrose, and different NaCl concentrations. Transport rates were calculated from the initial slopes and plotted against the Na^+ concentration in a Michaelis-Menten (*A*) or Lineweaver-Burk (*B*) plot. Data from two independent experiments are shown.

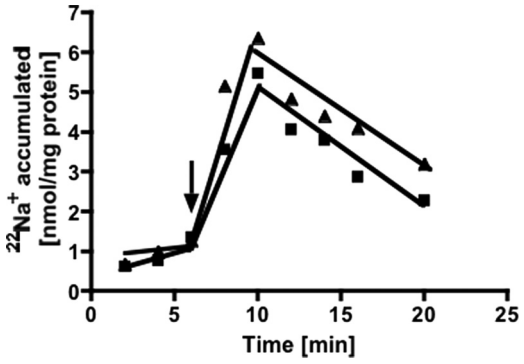

FIGURE 4. **$^{22}Na^+$ transport is electrogenic.** Membrane vesicles (protein concentration of 2.8 mg/ml) in Pipes/KOH buffer (pH 6.8) containing 25 mM $MgSO_4$, 420 mM sucrose, 1.9 mM NaCl, 150 mM KCl, and 17 μM valinomycin showed $^{22}Na^+$ transport upon addition of PP_i (*triangles*) and no addition of valinomycin (*squares*). The *arrow* indicates the addition of PP_i.

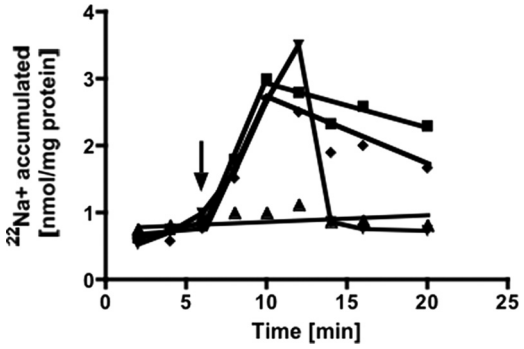

FIGURE 5. **$^{22}Na^+$ transport is a primary event.** Membrane vesicles (protein concentration of 2.8 mg/ml) in Pipes/KOH buffer (pH 6.8) containing 25 mM $MgSO_4$, 420 mM sucrose, and 1.9 mM NaCl showed $^{22}Na^+$ transport upon the addition of 1 mM PP_i (*squares*). ETH 2120 (100 μM) was added 6 min before (*triangles*) or 6 min after (*inverted triangles*) addition of PP_i. SF 6847 (100 μM) (*diamonds*) was added 6 min before the addition of PP_i. The *arrow* indicates the addition of PP_i.

lower PP_i concentrations, the Na^+ gradient established collapsed after some time, which may be due to PP_i depletion. There was a negligible activity at the lowest Na^+ concentration achieved in the assay (900 μM, taking into account the buffer, vesicles, and potassium pyrophosphate), but transport activity increased with increasing Na^+ concentration in a Michaelis-Menten fashion (Fig. 3*A*). The corresponding Lineweaver-Burk plot is shown in Fig. 3*B*. The K_m for Na^+ transport was determined to be 7.2 ± 1.4 mM, and the V_{max} was 3.6 ± 0.25 nmol/min/mg of protein. This gives a Na^+/PP_i ratio of 0.02.

The intravesicular Na^+ concentration in the IMVs (and thus the magnitude of the established Na^+ gradient) was also dependent on the concentration of Na^+. At 0.9 mM NaCl, a 10-fold accumulation was observed. Increasing Na^+ concentrations led to decreasing Na^+ gradients. At 1.9 mM NaCl, the accumulation factor was 9-fold, and at 40.9 mM NaCl, it was only 2.2-fold. Because the accumulation factor was higher at lower sodium concentrations, all subsequent experiments were performed in the presence of 1.9 mM NaCl.

It has been described previously that the PPase activity in *Rhodospirillum rubrum* and the activity of PPase isolated from mung beans are Mg^{2+}-dependent (19, 20). To test the effect of Mg^{2+} on the PP_i-dependent Na^+ transport at IMVs of *A. woodii*, IMVs had to be prepared in Mg^{2+}-free buffer. Unfortunately, when IMVs were prepared in the absence of $MgSO_4$, the yield was very low, and the activity was very low, indicating that $MgSO_4$ stabilizes the IMVs. When these IMVs were added to Mg^{2+}-free assay buffer, Na^+ transport (at 1.9 mM NaCl) was very low, with 0.004 nmol/min/mg of protein. The addition of Mg^{2+} to a final concentration of 25 mM stimulated Na^+ transport by 2000% to 0.08 nmol/min/mg of protein. When the Mg^{2+}-containing assay was supplemented with EDTA, Na^+ transport dropped to 0.01 nmol/min/mg of protein. These data show that PPase-driven Na^+ transport requires Mg^{2+}.

If transport of $^{22}Na^+$ is electrogenic, a membrane potential should be established that in turn should slow down $^{22}Na^+$ transport. To test this, we used valinomycin in combination with KCl to dissipate the potential ($\Delta\Psi$). KCl itself (0, 50, 100, and 150 mM) had no effect on Na^+ transport. However, in combination with valinomycin, $^{22}Na^+$ transport was stimulated slightly (Fig. 4). This experiment indicates that PP_i-driven $^{22}Na^+$ transport is electrogenic.

PP_i-dependent Na^+ transport should lead to the generation of a sodium ion potential that then could be used by the Na^+ F_1F_0-ATP synthase of *A. woodii* to synthesize ATP. If this is true, inhibition of the Na^+ F_1F_0-ATP synthase should lead to higher levels of $^{22}Na^+$ in the lumen of the vesicles. This was indeed observed. In the presence of the F_0-directed inhibitor *N*,*N*′-dicyclohexylcarbodiimide (1 mM, no extra sodium added to the assay), PP_i-driven accumulation of $^{22}Na^+$ was increased by 25%. However, the Na^+ transport rate was not affected.

Pyrophosphatase activity could be directly or indirectly (via a primary H^+ gradient in combination with a Na^+/H^+ antiporter) coupled to Na^+ transport. To discriminate between these possibilities, we used protonophores or sodium ionophores and analyzed their effect on $^{22}Na^+$ transport. The protonophore SF 6847 (100 μM) did not inhibit $^{22}Na^+$ accumulation (Fig. 5). The effectiveness of the uncoupler was ensured by its ability to dissipate an artificial ΔpH created by a NH_4^+ diffusion potential (21). The sodium ionophore ETH 2120 (100 μM) completely inhibited $^{22}Na^+$ accumulation; moreover, a previously established Na^+ gradient was dissipated immediately upon the addition of ETH 2120 (Fig. 5). These

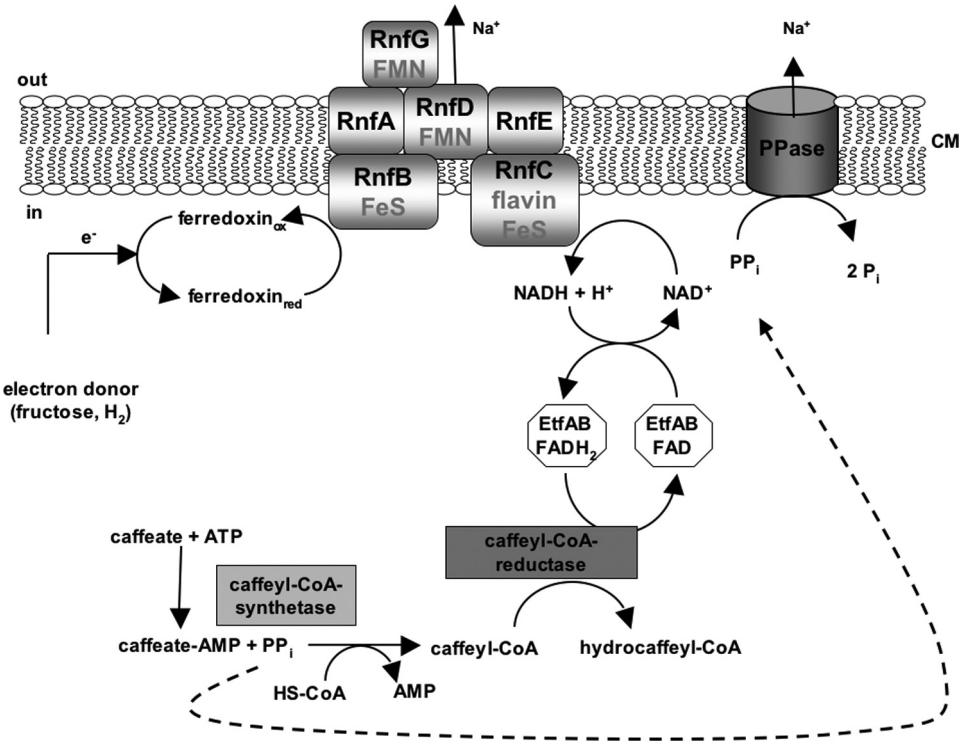

FIGURE 6. **Model of caffeate respiration in *A. woodii*.** Flow of electrons from electron donors (fructose or hydrogen) to the acceptor caffeate is shown. The PP_i generated by the caffeyl-CoA synthetase is used by the PPase to pump Na^+ across the membrane.

data demonstrate that $^{22}Na^+$ transport is directly linked to pyrophosphatase activity.

DISCUSSION

Pyrophosphatases are commonly found enzymes. Next to soluble pyrophosphatases, membrane-bound enzymes have been found in bacteria, archaea, and plants (22–25). It has been shown that membrane-bound PPases couple PP_i hydrolysis with proton or sodium ion transport (23, 26–29). Proton-pumping PPases acidify vacuoles in plants (22). In bacteria, they have been proposed to support energy conservation under conditions of energy deprivation (30, 31), and a light-induced maintenance of PP_i levels by PPase has been suggested based on experiments with *Rhodobacter capsulatus* (32). PP_i is a by-product of many biosynthetic processes for macromolecules, such as RNA and DNA synthesis, polysaccharide synthesis, formation of fatty acyl-CoA, and amino acid activation, and is formed in several reactions for substrate activation by anaerobic bacteria, *e.g.* activation of sulfate by sulfate-reducing bacteria or in activation of benzoate derivatives during anaerobic degradation of these compounds (23, 33).

Here, we have demonstrated a Na^+-pumping pyrophosphatase at IMVs of *A. woodii*. The coupling efficiency was low, indicating leakiness of the vesicle system. Additionally, a second non-Na^+-motive pyrophosphatase may contribute to PP_i hydrolysis activity. This enzyme may be membrane-attached and thus also explain the different K_m values for $^{22}Na^+$ transport and PP_i hydrolysis.

The overall ATP gain of caffeate respiration, as it is understood now, is very low. Electron flow from ferredoxin (−500 to −420 mV) to NAD^+ (−320 mV) is accompanied with a free energy change of only −35 to −19 kJ/mol, and therefore, the Fno/Rnf complex allows for the synthesis of about one-third to one-half of an ATP. Thus, 2–3 mol of hydrogen have to be oxidized to get 1 ATP. Therefore, its highly economic for the cells to save the energy stored in PP_i. The standard free energy stored in the PP_i bond is equivalent to −22 kJ/mol. Assuming a membrane potential of −200 mV, this would allow for translocation of 1 Na^+. Consequently, 3 mol of PP_i have to be hydrolyzed for the production of 1 mol of ATP. This is only a small amount of energy saved, but rationalizing that caffeate respiration is at the thermodynamic limit, this adds another piece to the overall energy balance. Additionally, energy may be conserved by electron bifurcation from NADH to ferredoxin in the process of caffeyl-CoA reduction and the subsequent Fno/Rnf complex-catalyzed ferredoxin oxidation (34, 15). Furthermore, in the steady state of caffeate respiration, the activation of caffeate is likely to be catalyzed by an energy-saving CoA loop from hydrocaffeyl-CoA to caffeate (35).

In summary, caffeate respiration involves an initial activation of the caffeate prior to its reduction by a AMP and PP_i, forming caffeyl-CoA synthetase, yielding caffeyl-CoA. The produced PP_i, as shown here, can be used by a membrane-bound pyrophosphatase to translocate Na^+ across the cytoplasmic membrane in *A. woodii*. Therefore, the energy stored in the PP_i bond is not lost but reinvested and conserved in a chemiosmotic Na^+ potential (Fig. 6).

REFERENCES

1. Müller, V., Imkamp, F., Rauwolf, A., Küsel, K., and Drake, H. L. (2004) in *Strict and Facultative Anaerobes: Medical and Environmental Aspects*

(Nakano, M. M., and Zuber, P., eds) pp. 251–281, Horizon Biosciences, Norfolk
2. Müller, V. (2003) *Appl. Environ. Microbiol.* **69,** 6345–6353
3. Schmidt, S., Biegel, E., and Müller, V. (2009) *Biochim. Biophys. Acta* **1787,** 691–696
4. Müller, V., Aufurth, S., and Rahlfs, S. (2001) *Biochim. Biophys. Acta* **1505,** 108–120
5. Heise, R., Müller, V., and Gottschalk, G. (1989) *J. Bacteriol.* **171,** 5473–5478
6. Heise, R., Müller, V., and Gottschalk, G. (1993) *FEMS Microbiol. Lett.* **112,** 261–267
7. Heise, R., Müller, V., and Gottschalk, G. (1992) *Eur. J. Biochem.* **206,** 553–557
8. Fritz, M., and Müller, V. (2007) *FEBS J.* **274,** 3421–3428
9. Müller, V., and Bowien, S. (1995) *Arch. Microbiol.* **164,** 363–369
10. Imkamp, F., Biegel, E., Jayamani, E., Buckel, W., and Müller, V. (2007) *J. Bacteriol.* **189,** 8145–8153
11. Imkamp, F., and Müller, V. (2002) *J. Bacteriol.* **184,** 1947–1951
12. Müller, V., Imkamp, F., Biegel, E., Schmidt, S., and Dilling, S. (2008) *Ann. N.Y. Acad. Sci.* **1125,** 137–146
13. Tschech, A., and Pfennig, N. (1984) *Arch. Microbiol.* **137,** 163–167
14. Biegel, E., and Müller, V. (2010) *Proc. Natl. Acad. Sci. U.S.A.,* **107,** 18138–18142
15. Biegel, E., Schmidt, S., Gonzáles, J. M., and Müller, V. (2011) *Cell Mol. Life Sci.* 10.1007/s00018-010-0555-8
16. Bradford, M. M. (1976) *Anal. Biochem.* **72,** 248–254
17. Heinonen, J. K., and Lahti, R. J. (1981) *Anal. Biochem.* **113,** 313–317
18. Pisa, K. Y., Huber, H., Thomm, M., and Müller, V. (2007) *FEBS J.* **274,** 3928–3938
19. Maeshima, M., and Yoshida, S. (1989) *J. Biol. Chem.* **264,** 20068–20073
20. Sosa, A., Ordaz, H., Romero, I., and Celis, H. (1992) *Biochem. J.* **283,** 561–566
21. Nakamura, T., Hsu, C., and Rosen, B. P. (1986) *J. Biol. Chem.* **261,** 678–683
22. Rea, P. A., and Poole, R. J. (1993) *Annu. Rev. Plant Physiol. Plant Mol. Biol.* **44,** 157–180
23. Maeshima, M. (2000) *Biochim. Biophys. Acta* **1465,** 37–51
24. Serrano, A., Perez-Castiñeira, J. R., Baltscheffsky, H., and Baltscheffsky, M. (2004) *J. Bioenerg. Biomembr.* **36,** 127–133
25. Docampo, R., de Souza, W., Miranda, K., Rohloff, P., and Moreno, S. N. (2005) *Nat. Rev. Microbiol.* **3,** 251–261
26. Belogurov, G. A., Malinen, A. M., Turkina, M. V., Jalonen, U., Rytkönen, K., Baykov, A. A., and Lahti, R. (2005) *Biochemistry* **44,** 2088–2096
27. Malinen, A. M., Belogurov, G. A., Baykov, A. A., and Lahti, R. (2007) *Biochemistry* **46,** 8872–8878
28. Baltscheffsky, M., Schultz, A., and Baltscheffsky, H. (1999) *FEBS Lett.* **457,** 527–533
29. Malinen, A. M., Baykov, A. A., and Lahti, R. (2008) *Biochemistry* **47,** 13447–13454
30. Skulachev, V. P. (1977) *FEBS Lett.* **74,** 1–9
31. Nyren, P., and Strid, A. (1991) *FEMS Microbiol. Lett.* **77,** 265–269
32. Nore, B. F., Nyren, P., Salih, G. F., and Strid, A. (1990) *Photosynth. Res.* **24,** 75–80
33. Schöcke, L., and Schink, B. (1998) *Eur. J. Biochem.* **256,** 589–594
34. Herrmann, G., Jayamani, E., Mai, G., and Buckel, W. (2008) *J. Bacteriol.* **190,** 784–791
35. Hess, V., Vitt, S., and Müller, V. (2011) *J. Bacteriol.*, in press